Asian Journal of Information Technology 15 (1): 162-168, 2016
ISSN: 1682-3915


# Design and Simulation of an Advanced Rectifier Stage Topology with Maximum Power Point Tracking for Hybrid Energy Systems

[1]C. Kathirvel, [2]M. Gopinath, [3]K. Porkumaran and [2]S. Jagannathan
[1]Department of Electrical and Electronics Engineering,
Sri Ramakrishna Engineering College, Coimbatore, India
[2]Department of Electrical and Electronics Engineering,
Institute of Technology, Coimbatore, India
[3]Institute of Technology, Coimbatore, Tamil Nadu, India

**Abstract:** With the concern regarding the state of our deteriorating planet, environmentally friendly solutions are becoming more prominent. This study presents a new system configuration of the front-end rectifier stage consisting of CUK-SEPIC fused converter for a hybrid wind/photovoltaic energy system. The configuration allows the two sources to supply the load separately or simultaneously depending on the availability of the energy sources. With this converter integration, additional input filters are not necessary to filter out high frequency harmonics. The fused multi input rectifier stage also allows Maximum Power Point Tracking (MPPT) to be used to extract maximum power from the wind and sun when it is available. A microcontroller based control method is used for the Maximum Power Point Tracking (MPPT) of the energy system. For the reduction of tracking time, Fuzzy Logic Control algorithm is implemented with the embedded microcontroller for improved performance. Operational analysis of the proposed system will be discussed in this study. Simulation results are given to highlight the merits of the proposed circuit.

**Key words:** Rectifier topology, MPPT, fuzzy logic, hybrid energy systems, CUK-SEPIC

## INTRODUCTION

The increasing concern of global warming and the depletion of fossil fuel reserves force to look at sustainable energy solutions to preserve the earth for the future generations. Other than hydro power, photovoltaic and wind energy holds the most potential to meet our energy demands. The wind energy is capable of supplying large amounts of power but its presence is highly unpredictable. The common inherent drawback of wind and photovoltaic systems are the intermittent natures that make them unreliable. By combining these two intermittent sources and by incorporating Maximum Power Ppoint Tracking (MPPT) algorithms, the system's power transfer efficiency and reliability can be improved for the system. Several hybrid wind/PV power systems with MPPT control have been proposed and discussed in researcher (Ahmed *et al*., 2008; Chen *et al*., 2007; Das *et al*., 2005). Most of the systems in literature use a separate DC/DC boost converter connected in parallel in the rectifier stage to perform the MPPT control for each of the renewable energy sources. A multi input structure has been suggested by (Chen *et al*., 2007) combines the sources from the DC-end while still achieving MPPT for each renewable source. The structure proposed by (Chen *et al*., 2007) is a fusion of the buck and buck-boost converter. The systems in literature require passive input filters to remove the high frequency current harmonics injected into wind turbine generators.

An alternative multi-input rectifier structure is proposed for hybrid wind/solar energy systems. The proposed design is a fusion of the CUK and SEPIC converters. The features of the proposed topology are: eliminates the need for separate input filters for PFC. It can support step up/down operations for each renewable source. MPPT can be realized for each source. Individual and simultaneous operation is supported. Simulation results are provided to verify with the feasibility of the proposed system.

## MATERIALS AND METHODS

**Proposed multi-input rectifier stage:** A system diagram of the proposed rectifier stage of a hybrid energy system

**Corresponding Author:** C. Kathirvel, Department of Electrical and Electronics Engineering, Sri Ramakrishna Engineering College, Coimbatore, Tamil Nadu, India

is shown in Fig. 1 where one of the inputs is connected to the output of the PV array and the other input connected to the output of a generator. The fusion of the two converters is achieved by reconfiguring the two existing diodes from each converter and the shared utilization of the CUK output inductor by the SEPIC converter. This configuration allows each converter to operate normally individually in the event that one source is unavailable. In the case when only the wind source is available, D1 turns off and D2 turns on; the proposed circuit becomes a SEPIC converter and the input to output voltage relationship is given by Eq. 1. On the other hand, if ony the PV source is available, then D2 turns off and D1 will always be on and the circuit becomes a CUK converter. The input to output voltage relationship is given by Eq. 2. In both cases, both converters have step-up/down capability which provide more design flexibility in the system if duty ratio control is utilized to perform MPPT control:

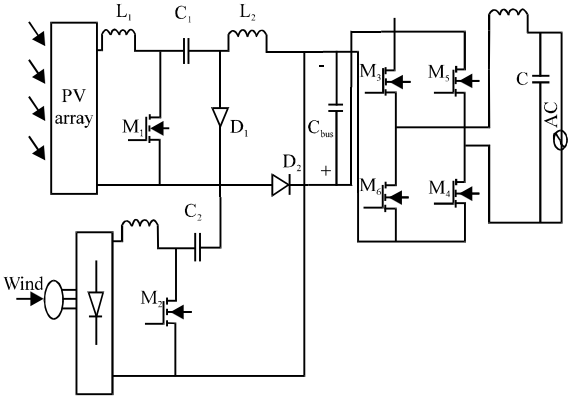


Fig. 1: Proposed rectifier stage for a Hybrid wind/PV system

$$\frac{V_{dc}}{V_w} = \frac{d_2}{1-d_2} \quad (1)$$

$$\frac{V_{dc}}{V_{pv}} = \frac{d_2}{1-d_1} \quad (2)$$

Figure 2 illustrates the various switching states of the proposed converter. If the turn on duration of M1 is longer than M2, then the switching states will be state a, b, d. Similarly, the switching states will be state a, c, d. The inductor current waveforms of each switching state are given in Fig. 3.

The mathematical expression that relates the total output voltage and the two input sources is given by Eq. 3.

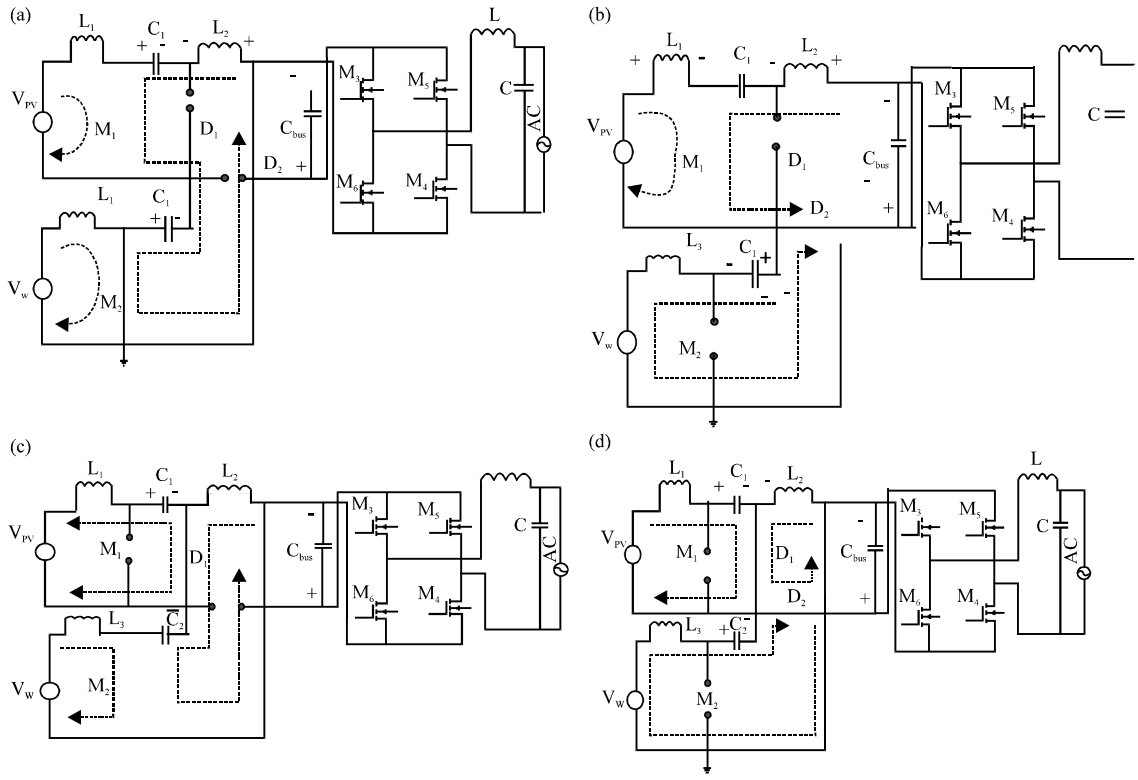


Fig. 2: a-d) Switching states within a switching cycle

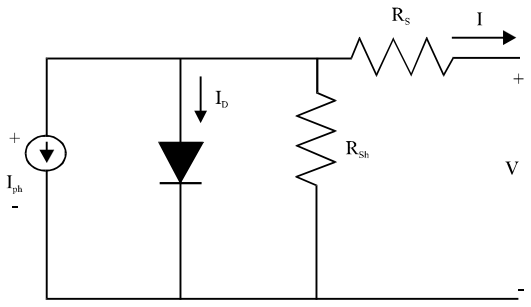


Fig. 3: PV cell equivalent circuit

$$V_{dc} = \frac{d_1}{1-d_1} V_{PV} + \frac{d_2}{1-d_2} V_W \quad (3)$$

It is observed that $V_{dc}$ is simply the sum of the two output voltages of the CUK and SEPIC converter. This further implies that $V_{dc}$ can be controlled by $d_1$ and $d_2$ individually or simultaneously.

The voltage stress for the two switches is given by Eq. 4 and 5, respectively. As for the current stress, it is observed from Fig. 3 that the peak current always occurs at the end of the on-time of the MOSFET. Both the Cuk and SEPIC MOSFET current consists of both the input current and the capacitors ($C_1$ or $C_2$) current. $L_{eq1}$ and $L_{eq2}$, given by Eq. 6 and 7, represent the equivalent inductance of CUK and SEPIC converter, respectively.

$$V_{ds1} = V_{pv}\left(1 + \frac{d_1}{1-d_1}\right) \quad (4)$$

$$V_{ds2} = V_{pv}\left(1 + \frac{d_2}{1-d_2}\right) \quad (5)$$

$$L_{eq1} = \frac{L_1 L_2}{L_1 + L_2} \quad (6)$$

$$L_{eq2} = \frac{L_3 L_2}{L_3 + L_2} \quad (7)$$

The dc bus voltage, $V_{dC}$ will be regulated by the dc/ac inverter with Sinusoidal PWM (SPWM) control to achieve the input output power-flow balance. The dc/ac inverter will inject a sinusoidal current into the ac mains. The SPWM gate signals of switches $M_3$ through $M_6$ for producing sinusoidal ac current is generated by the microcontroller where the amplitude of the ac current is determined by the error signal of the measured dc bus voltage $V_{DC}$ and the reference one, $V_{DC, ref}$. If the measured dc bus voltage is less than the reference value, then the amplitude of the ac output current will be decreased in order to increase the dc bus voltage. On the contrary if the dc bus voltage is higher than the reference one, then, the amplitude of the ac output current will be decreased. On the other point of view, the dc bus voltage is regulated by the dc-ac inverter and the input-output power balance can be achieved.

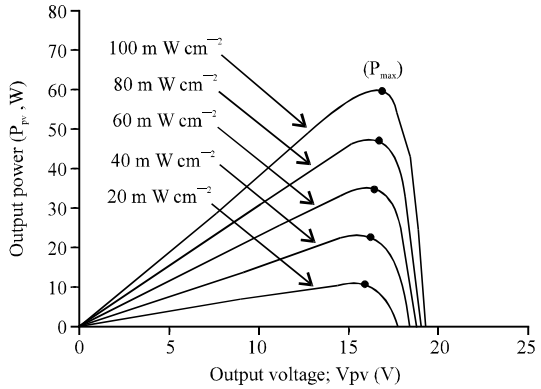


Fig. 4: Typical output power characteristic curve of the pv array under different insolation

**MPPT control of proposed circuit:** A common inherent drawback of wind and PV systems is the intermittent nature of their energy sources. These drawbacks tend to make these renewable systems inefficient. By incorporating Maximum Power Point Tracking (MPPT) algorithms, the systems' power transfer efficiency can be improved significantly (Hsiao and Chen, 2002; Hui *et al*., 2010). The PV array is constructed by many series or parallel connected solar cells. Each solar cell is form by a PN junction semiconductor which can produce currents by the photovoltaic effect. A PV cell is a diode of a large-area forward bias with a photo voltage and the equivalent circuit is shown by Fig. 4. The current-voltage characteristic of a solar cell is given by Eq. 8 and 9:

$$I = I_{ph} - I_D \quad (8)$$

$$I = I_{ph} - I_0[\exp(qV + R_{S1}/AK_{BT} - 1] - V + R_{S1}/R_{sh} \quad (9)$$

Where:

$I_{ph}$ = Photocurrent
$I_D$ = Diode current
$I_0$ = Saturation current
A = Ideality factor
q = Electronic charge 1.6×10-9
$k_B$ = Boltzmann's gas constant (1.38×10-23)
T = Cell temperature

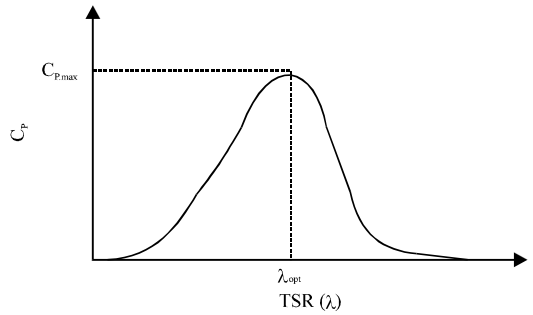


Fig. 5: Power coefficient curve for a typical wind turbine

$R_s$ = Series resistance
$R_{sh}$ = Shunt resistance
I = Cell current
V = Cell voltage

Typical output power characteristic curves for the PV array under different insolation are shown in Fig. 5. It can be seen that a maximum power point exists on each output power characteristic curve. Therefore, to utilize the maximum output power from the PV array, an appropriate control algorithm must be adopted.

The wind turbine's power characteristic can be described by the power of the wind which can be derived by Eq. 10:

$$P_{wind} = \frac{1}{2}\rho A C_p(\lambda\beta)\, v_w^3 \quad (10)$$

Where:

$\rho$ = Air density
A = Rotor swept area
$C_{p(\lambda,\beta)}$ = Power coefficient function
$\lambda$ = Tip speed ratio
$\beta$ = Pitch angle
$v_w$ = Wind speed

The power Coefficient ($C_p$) is a nonlinear function that represents the efficiency of the wind turbine to convert wind energy into mechanical energy. It is dependent on two variables, the Tip Speed Ratio (TSR) and the pitch angle. The TSR, $\lambda$ refers to a ratio of the turbine angular speed over the wind speed. The mathematical representation of the TSR is given by (Eq. 11). The pitch angle, $\beta$ refers to the angle in which the turbine blades are aligned with respect to its longitudinal axis:

$$\lambda = \frac{R_b}{v_w} \quad (11)$$

Where:

R = Turbine radius
$\omega_b$ = Angular rotational speed

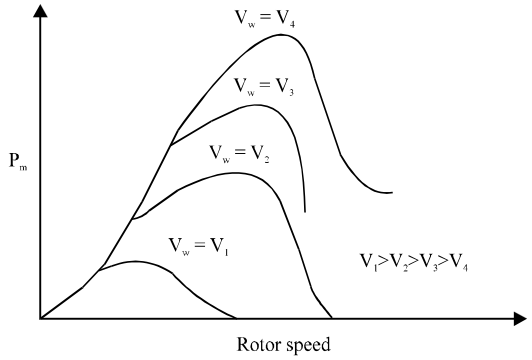


Fig. 6: Power curves for a typical wind turbine

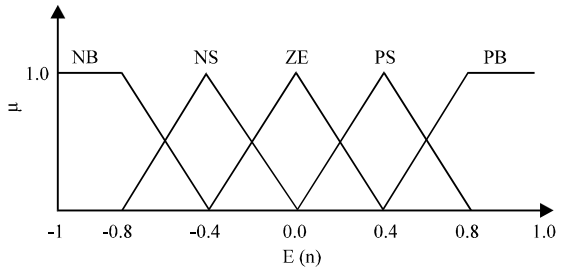


Fig. 7: The relationship between linguistics variable and error

Figure 5 and 6 are illustrations of a power coefficient curve and power curve for a typical fixed pitch horizontal axis wind turbine. It can be seen from Fig. 6 and 7 that the power curves for each wind speed has a shape similar to that of the power coefficient curve. Because the TSR is a ratio between the turbine rotational speed and the wind speed, it follows that each wind speed would have a different corresponding optimal rotational speed that gives the optimal TSR. For each turbine there is an optimal TSR value that corresponds to a maximum value of the power coefficient ($C_{p,max}$) and therefore the maximum power. Therefore by controlling rotational speed (by means of adjusting the electrical loading of the turbine generator) maximum power can be obtained for different wind speeds. Due to the similarities of the shape of the wind and PV array power curves, a similar maximum power point tracking scheme is often applied to these energy sources to extract maximum power.

Microcontrollers have made using fuzzy logic control popular for MPPT over last decade. For the reduction of tracking time, Fuzzy Logic Control algorithm is implemented with the embedded microcontroller for improved performance compared compared to conventional techniques in power efficiency and swift maximum power point tracking.

Fuzzy logic control generally consists of three stages: fuzzification, rule base table lookup and defuzzification.

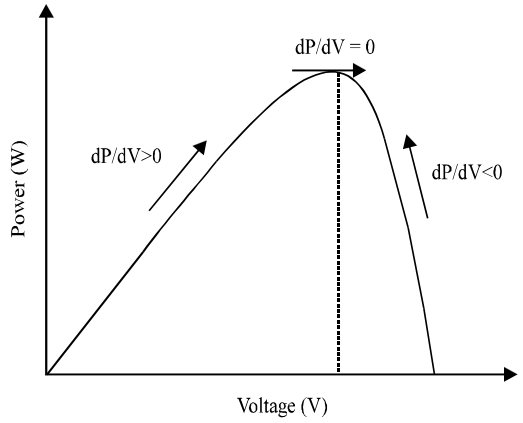


Fig. 8: The P-V characteristic of a PV module

During fuzzification, numerical input variables are converted into linguistic variables based on a membership function. The inputs to a MPPT fuzzy logic controller are usually an error E and a change of error ΔE as given in Eq. 12 and 13, respectively.

$$E(n)=\frac{P(n)-P(n-1)}{V(n)-V(n-1)} \quad (12)$$

$$\Delta E(n)=E(n)-E(n-1) \quad (13)$$

The E and ΔE are calculated and converted to the linguistic variables during fuzzification. Linguistic variables are non precise variables that often convey a surprising amount of information. To simplify the control calculation, the values of error E and change of error ΔE can be normalized with (Eq. 14) before fuzzification process:

$$Y_S=\begin{cases}-1, & Y<-Y^*\\ \dfrac{Y}{Y^*}, & Y<Y^*\\ 1, & Y>Y^*\end{cases} \quad (14)$$

where, $Y^* = Y_{max}$ so the scopes of error E and change of error ΔE will be [-1, 1]. Figure 7 shows the relations between measured error and the linquistive term such as positive small, positive medium and positive big. At some point, the error is positive small and at some point the error is positive big the space between positive big and positive small indicates an error that is, to some degree, a bit of both. The horizontal axis in the following graph shows the measured or crisp value of error. The vertical axis describes the degree to which a linguistic variable fits with the crisp measured data.

The characteristics of a PV system vary with temperature and insolation. So, the MPPT controller is also required to track the new modified maximum power point in its corresponding curve whenever, temperature and/or insolation variation occurs. The MPPT algorithm employed based on voltage and power feedback control approach, with the step size being dependant on the slope of the Power vs Voltage (P-V) curve as shown in Fig. 8. The slope of the PV array power curve is zero at the MPP, increasing on the left of the MPP and decreasing on the right-hand side of the MPP. The basic equations of this method are as follows:

Table 1: Fuzzy rule base tablee

| E | NB | NS | ZE | PS | PB |
|---|---|---|---|---|---|
| NB | ZE | ZE | NB | NB | NB |
| NS | ZE | ZE | NS | NS | NS |
| ZE | NS | ZE | ZE | ZE | PS |
| PS | PS | PS | PS | ZE | ZE |
| PB | PB | PB | PB | ZE | ZE |

$$\frac{dP}{dV}=0, \text{ at MPP} \quad (15)$$

$$\frac{dP}{dV}>0, \text{ Operation point on the left of MPP} \quad (16)$$

$$\frac{dP}{dV}<0, \text{ Operation point on the right of MPP} \quad (17)$$

where, P and V are the PV array output power and voltage, respectively. power point. The designed controller regulates the converter output voltage by varying duty cycle of the PWM signal using Maximum Power Point (MPP) algorithm and it maximizes the output power extracted from Photovoltaic array. The fuzzy logic controller output is typically a change in duty ratio ΔD of the power converter. The linguistic variables assigned to ΔD for the different combinations of E and ΔE as shown in Table 1. If, for example, the operating point is far to the left of the MPP as shown in Fig. 8 that is E is PB and ΔE is ZE, then we want to largely increase the duty ratio that is ΔD should be PB to reach the MPP.

The final step in the fuzzy logic controller is to combine the fuzzy output into a crisp systems output. The result of the defuzzification has to be a numeric value which determines the change of duty cycle of the PWM signal used to drive the MOSFET. There are various methods to calculate the crisp output of the system.

## RESULTS AND DISCUSSION

In this study, simulation results from MATLAB Simulink Version R2011a is given to verify that the proposed multi-input rectifier stage can support individual as well as simultaneous operation. The simulation is done for, when only solar is available, only wind is available and when both the energy sources are available. The

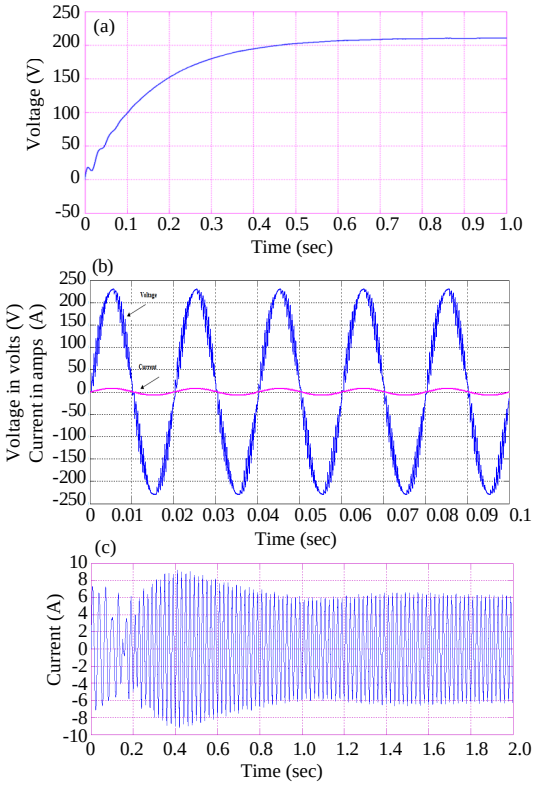


Fig. 9: Waveforms of the proposed system when only PV panel is supplying the power: a) DC Bus Voltage Waveform; b) Inverter output voltage and current waveform; c) Expanded ac output current waveform

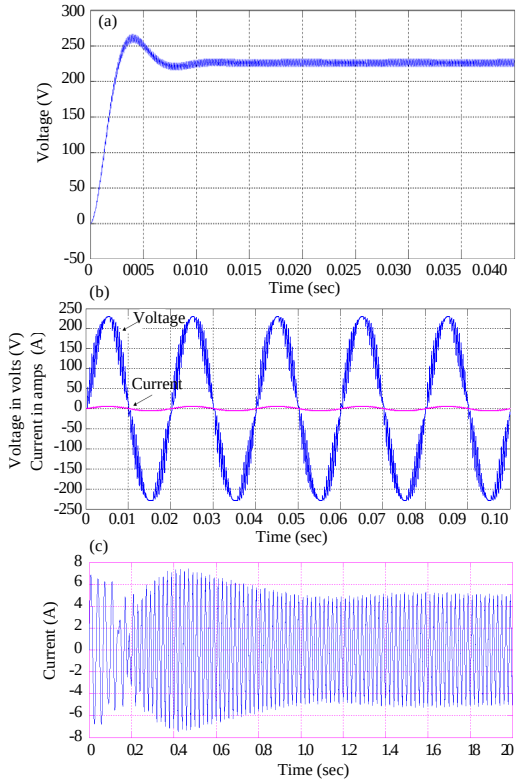


Fig. 10: Waveforms of the proposed system when only wind turbine is supplying the power: a) DC bus voltage Waveform; b) Inverter output voltage and current waveform; c) Expanded ac output current waveform

rectifier DC output voltage is inverted through a full bridge PWM inverter which uses Sinusoidal Pulse Width Modulation (SPWM). Circuit parameters are given as:

- The PV panel voltage, $V_{pv}$ = 60 V
- The rectified output voltage of $V_W$ = 280 V
- The wind generator
- Switching frequency of $M_1$ and $M_2$ =10 kHz
- Switching frequency of $M_3$-$M_6$ = 5 kHz

The inductor and capacitor values of the Cuk and SEPIC Converter are given below:

- Inductor $L_1$ = 30 mH
- Inductor $L_2$ = 6 mH
- Inductor $L_3$ = 6 mH
- Capacitor $C_1$ = 330 μH
- Duty Cycle $D_{M1}$ = 0.79
- Duty Cycle $D_{M2}$ = 0.48
- Filter Inductance L = 10 mH
- Filter Capacitance C = 6.3 nF

The SIMULINK block of the rectifier topology with MPPT consists of a PV array model, wind turbine with a PMSG, CUK and SEPIC fused rectifier stage, the MPPT block, single phase full bridge PWM inverter voltage and current measurement block. The gate pulse of inverter switches are controlled by Sinusoidal Pulse Width Modulation (SPWM).

Figure 9a shows the waveforms of the dc bus voltage when only the PV array is connected to the proposed rectifier topology. The ac output voltage and current waveforms of the proposed system is shown in Fig. 9b and the expanded current waveform is shown in Fig. 9c. The output current obtained is 6 Amperes (A).

Figure 10a shows the waveforms of the dc bus voltage when only wind turbine is connected to the proposed rectifier topology. The ac output voltage and current waveforms of the proposed system is shown in Fig. 10b and the expanded current waveform is shown in Fig. 10c. In this case, the output current obtained is 4.7 Amperes (A) which is less than that obtained when PV array is connected to the system.

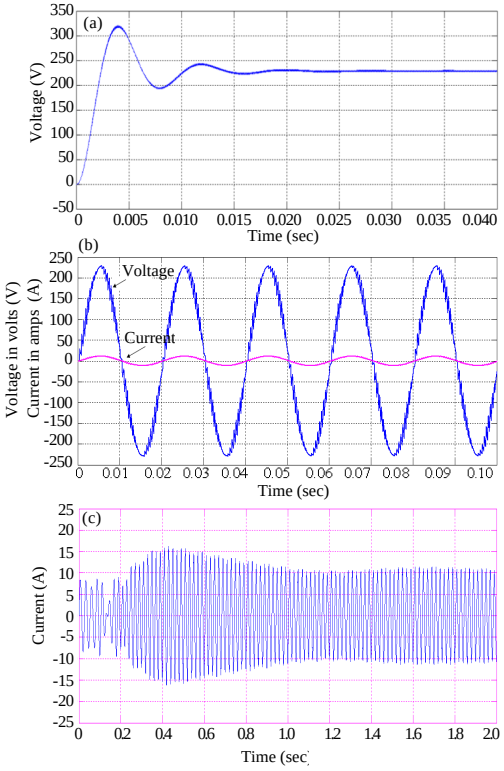


Fig. 11: Waveforms of the proposed system when both PV panel and wind turbine is supplying the power: a) DC Bus voltage waveform; b) Inverter output voltage and current waveform; c) Expanded ac output current waveform

Figure 11a shows the waveforms of the dc bus voltage when both PV panel and wind turbine is connected to the proposed rectifier topology. The ac output voltage and current waveforms of the proposed system is shown in Fig. 11b and the expanded current waveform is shown in Fig. 11c. In this case, the output current obtained is 9.4 Amperes (A) which is more than that obtained when either PV panel or wind turbine is connected to the system.

## CONCLUSION

An advanced rectifier stage topology was designed and simulated using MATLAB Simulink Version R2011a and the results have been presented to demonstrate the proposed rectifier stage topology. The simulation results shows that individual or simultaneous operation is possible to give a constant output voltage but slight variations in power. In this proposed system, additional input filters are not necessary to filter out high frequency harmonics. Both renewable sources can be stepped up/down (supports wide ranges of PV and wind input). Individual and simultaneous operation is supported. The reduced number components reduce the complexity of the system and hence the cost.

## REFERENCES

Ahmed, N.A., M. Miyatake and A.K. Al-Othman, 2008. Power fluctuations suppression of stand-alone hybrid generation combining solar photovoltaic/wind turbine and fuel cell systems. Energy Convers. Manage., 49: 2711-2719.

Chen, Y.M., Y.C. Liu, S.C. Hung and C.S. Cheng, 2007. Multi-input inverter for grid-connected hybrid PV/wind power system. Power Electr. IEEE. Trans., 22: 1070-1077.

Das, D., R. Esmaili, L. Xu and D. Nichols, 2005. An optimal design of a grid connected hybrid wind/photovoltaic/fuel cell system for distributed energy production. Proceedings of the 31st Annual Conference of IEEE Industrial Electronics Society, November 6-10, 2005, Raleigh, North Carolina, pp: 2499-2504.

Hsiao, Y.T. and C.H. Chen, 2002. Maximum power tracking for photovoltaic power system. Proceeding of the 37th IAS Annual Meeting Conference Record of the Industry Applications Conference, 2002, October 13-18, 2002, IEEE, Pittsburgh, PA, USA., pp: 1035-1040.

Hui, J., A. Bakhshai and P.K. Jain, 2010. A hybrid wind-solar energy system: A new rectifier stage topology. Proceeding of the 2010 Twenty-Fifth Annual IEEE Conference Applied Power Electronics and Exposition (APEC), February 21-25, 2010, IEEE, Palm Springs, CA, pp: 155-161.